Electronic Spectrum of Crystalline Copper*

F. M. MUELLER† AND J. C. PHILLIPS‡
Department of Physics and Institute for the Study of Metals, The University of Chicago, Chicago, Illinois
(Received 26 September 1966)

The optical spectrum of Cu is calculated in the random-phase approximation. Energy levels and model wave functions are obtained from Mueller's combined interpolation scheme. It is shown how oscillator strengths can be obtained throughout the Brillouin zone to an accuracy of about 20%. The optical energy differences and oscillator strengths have been computed from a Monte Carlo sample of 2716 independent points distributed throughout the Brillouin zone. The smoothed spectrum is in good agreement with the experimental spectrum above 4 eV. The second peak in the interband spectrum near 5 eV is assigned to conduction-band ($L_{2'}$) → conduction-band (L_1) transitions, in agreement with the suggestion of Beaglehole. It is proposed that the large peak near 2 eV should be regarded as a virtual exciton resonance induced by final-state vertex corrections.

I. INTRODUCTION

THE electronic structures of the noble metals at and near the Fermi energy E_F have been determined with great precision by Fermi-surface studies of extremal areas A (de Hass–van Alphen effect[1–3]) and extremal cyclotron masses (dH–vA and Azbel-Kaner effects[4]). These studies show that in this energy region the one-electron band structure calculated either by the augmented-plane-wave (APW) method[5] or the Green's-function method[6] is in extremely good agreement with experiment; in fact, the one-electron Fermi radii k_F agree to within 1%, which is the limit of error imposed by conversion[7] of areas to radii. After allowance for electron-phonon enhancement, satisfactory agreement is also obtained for the effective masses, which represent $(\partial A/\partial E)$ evaluated at $E=E_F$.

In systems such as the noble metals (and also transition metals) where d-electron interactions are expected to be larger than the calculated width of the one-electron d bands, such agreement would surprise us had not Landau pointed out that because of phase-space considerations one-electron concepts are still valid sufficiently close to E_F. Thus Migdal showed[8] that the Fermi surface itself is still a well-defined quantity even in strongly interacting systems.

The purpose of this paper is to investigate the validity of the single-particle model well away from E_F by studying the optical absorption spectrum. This consists of two parts: That arising from intraband (Drude) currents, and the interband current. We focus our attention on the latter; its contribution to the dielectric response of the crystal can be computed in the random-phase approximation if we assume that the dominant term arises from direct interband transitions, i.e., those transitions which conserve crystal momentum, when the momentum of the absorbed photon may be neglected. The imaginary part ϵ_2 of the dielectric response is then given by[9]

$$\epsilon_2=\frac{4\pi^2e^2\hbar^2}{3m^2\omega^2}\sum_{m,n}\int_{\text{B.z.}}\frac{2}{(2\pi)^3}d\mathbf{k}\,|\mathbf{P}_{mn}|^2\times\delta(E_n-E_m+h\omega), \quad (1.1)$$

where m labels occupied states, n labels unoccupied states, and the interband oscillator strength is

$$\mathbf{P}_{mn}=\frac{\hbar}{\Omega i}\int\Psi_{\mathbf{k}m}{}^*\nabla\Psi_{\mathbf{k}n}d\tau \quad (1.2)$$

integrated over the unit cell of volume Ω.

As we have remarked above, the one-electron band structure calculated for Cu by Burdick is in excellent quantitative agreement with Fermi-surface measurements. We can therefore test the validity of the single-particle model by calculating (1.1) from energy levels and wave functions obtained from Burdick's crystal potential. However, the completion of this program, which is simple in principle, is complicated in practice by two factors. The phase-space sum over frequencies cannot be performed analytically for the entire Brillouin zone (B.z.) even if the assumption (which is often made) that the oscillator strengths (1.2) are constant were to be correct. Partial evaluation of (1.1) by graphical techniques in neighborhoods of the zone, or replacement of the actual energies by analytic approximations, cannot provide a valid test of the model.

The phase-space sums can be evaluated in general by a Monte Carlo method based on the combined interpolation scheme developed earlier[10] with a view to solving problems of this type. Our interpolation scheme uses

* Supported in part by the National Science Foundation and the U. S. Army Research Office (Durham).
† Present address: Argonne National Laboratory, Argonne, Illionis.
‡ Alfred P. Sloan Fellow.
[1] D. Shoenberg, Phil. Trans. Roy. Soc. (London) **A255**, 85 (1962); A. S. Joseph *et al.*, Phys. Rev. **148**, 569 (1966): Cu.
[2] D. Shoenberg (Ref. 1); A. S. Joseph and A. C. Thorsen, Phys. Rev. **138**, A1159 (1965): Ag.
[3] D. Shoenberg (Ref. 1); A. S. Joseph and A. C. Thorsen, Phys. Rev. **140**, A2046 (1965): Au.
[4] A. F. Kip, D. N. Langenberg, and T. W. Moore, Phys. Rev. **124**, 359 (1961).
[5] G. A. Burdick, Phys. Rev. **129**, 138 (1963).
[6] B. Segall, Phys. Rev. **125**, 109 (1962).
[7] E. Zornberg and F. M. Mueller, Phys. Rev. **151**, 557 (1966).
[8] A. B. Migdal, Zh. Eksperim. i Teor. Fiz. **32**, 399 (1957) [English transl.: Soviet Phys.—JETP **5**, 333 (1957)].
[9] H. Ehrenreich and M. H. Cohen, Phys. Rev. **115**, 786 (1959).
[10] F. M. Mueller, Phys. Rev. (to be published).

9×9 matrices to give an abstract representation of both the d bands and the low-lying conduction bands. The matrix elements are simple analytic functions of $\mathbf{k}$; E appears explicitly in the matrix and only along the diagonal. Burdick's eigenvalues, calculated on a coarse mesh of 89 points in 1/48 of the Brillouin zone, are reproduced with an rms error of less than 0.1 eV (i.e., less than lifetime broadening in the energy range of interest, and probably also less than the uncertainties in several levels based on unknown limitations in the determination of the crystal potential).

An intrinsic feature of the combined interpolation scheme which is essential to the success of the present calculations is that the parameters and form factors there introduced have real physical significance; no unphysical quantities appear in the scheme to compensate for, e.g., excessively large hybridization parameters. This feature is essential when we come to evaluate (1.2) throughout the Brillouin zone. At first sight our abstract interpolation scheme yields eigenfunctions in terms of linear combinations of model functions with no means available to obtain the actual Bloch functions which would emerge from an APW calculation. However, by accepting an uncertainty in $|P|^2$ of about 10%, we find that the situation is just the reverse of this. If APW eigenfunctions were available throughout the Brillouin zone, they would still make the determination of (1.2) difficult in practice. This is because plane waves in the muffin-tin region outside the inscribed spheres do not constitute an orthonormal basis set, nor are they eigenfunctions of $\mathbf{P}$. On the other hand, by making use of certain identities based on Phillips's modification of $\mathbf{k}\cdot\mathbf{p}$ perturbation theory (his partial-sum rules[11]), we have found that $\mathbf{P}_{mn}$ can be determined both for conduction-band → conduction-band and d-band → conduction-band transitions, both accurately and simply, directly from the model eigenfunctions without adjustment of parameters and in a way subject to internal verification. This permits an absolute calculation of the optical absorption, within the framework of the one-electron random-phase approximation.

In Sec. II we describe the most subtle aspect of our calculations, the determination of $\mathbf{P}_{mn}$ throughout the Brillouin zone. In Sec. III we present the results for the composite $\epsilon_2(\omega)$ based on all pairs of bands. Structure in the spectrum is analyzed by decomposing not into pairs of band (as Brust did[12] for diatomic Si and Ge), but according to the change in the quantum number m_k discussed in a preceding paper.[13] In Sec. IV the results of the present work are compared with approximate graphical treatments by other workers.[14–16] It is shown that due to the inherent limitations of the graphical approach much of the preceding work has only qualitative significance. Our results are summarized in Sec. V.

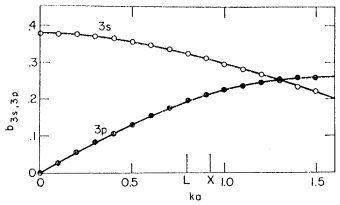

FIG. 1. The orthogonality form factors b_{3s} and b_{3p} in Cu as calculated from atomic wave functions (Ref. 18) are plotted as functions of ka, where a is the lattice constant.

II. DETERMINATION OF OSCILLATOR STRENGTHS

Consider first the determination of oscillator strengths at points of high symmetry such as X and L. We expand the Bloch functions in (1.2) in terms of model basis functions $\phi_{\mathbf{k}m}$:

$$\Psi_{\mathbf{k}n}=\sum_m a_{\mathbf{k}n}{}^m\phi_{\mathbf{k}m}, \tag{2.1}$$

where $\mathbf{a}_\mathbf{k}$ represents the eigenvector derived from the solution of the secular equation involving the model Hamiltonian at the point $\mathbf{k}$. Because the model Hamiltonian reproduces in a simple and natural way Burdick's band structure for Cu with high accuracy, we believe that $\mathbf{a}_\mathbf{k}$ is obtained accurately. We verify this point by checking below the internal consistency of our oscillator strengths.

To calculate momentum matrix elements, we retain the assumption that the d states can be represented as products of cubic harmonics with a common radial function (ansatz of spherical isotropy). The conduction basis functions are treated as single plane waves implicitly orthogonalized to $3s$ and $3p$ core states. Correction terms associated with more tightly bound core states were found[17] to be small in Si.

Both d states and conduction states can be classified using the quantum number m_k discussed in a preceding paper.[13] When $\mathbf{p}$ is parallel to $\mathbf{k}$ we excite transitions with $\Delta m_k=0$ whereas when $\mathbf{p}$ is perpendicular to $\mathbf{k}$ we excite transitions with $|\Delta m_k|=1$. The simplest case, where m_k is a good quantum number, is X. There the lowest conduction-band state has the form

$$|X_{4'}\rangle=\frac{1}{\sqrt{2}}\frac{1}{C_X}[\exp(i\mathbf{X}\cdot\mathbf{r})-\exp(-i\mathbf{X}\cdot\mathbf{r}) -2\langle p|\mathbf{X}\rangle|p\rangle], \tag{2.2}$$

where C_X is a normalizing factor involving the orthogonality form factor $\langle p|\mathbf{X}\rangle$ between the $3p$ core state and the plane-wave $|\mathbf{X}\rangle$. The $3s$ and $3p$ core states lie

[11] J. C. Phillips, Phys. Rev. (to be published).
[12] D. Brust, Phys. Rev. **134**, A1337 (1964).
[13] J. C. Phillips and F. M. Mueller (to be published).
[14] H. Ehrenreich and H. R. Philipp, Phys. Rev. **128**, 1622 (1962), referred to as EP.
[15] B. R. Cooper, H. Ehrenreich, and H. Philipp, Phys. Rev. **138**, A494 (1965), referred to as CEP.
[16] E. Haga and H. Okamoto, J. Phys. Soc. Japan **20**, 1610 (1965); E. Haga (to be published).
[17] L. Kleinman and J. C. Phillips, Phys. Rev. **118**, 1153 (1960).

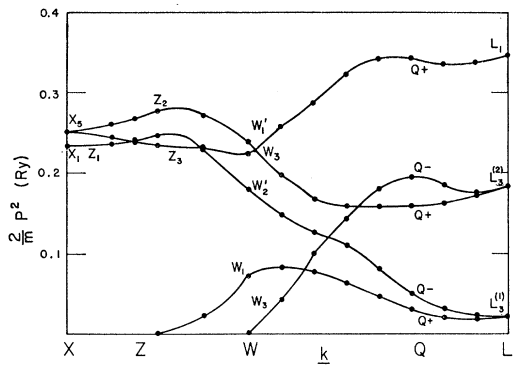

FIG. 2. The interband momentum matrix elements P_{ij}^2 scaled by $2/m$ are shown in Ry plotted against $\mathbf{k}$ around the outside of the Brillouin zone from X to W to L. Here i ranges over the first 5 d bands, while j is fixed to be the lowest conduction band. Thus the oscillator strengths at X correspond to $X_5 \rightarrow X_{4'}$ and $X_5 \rightarrow X_1$ transitions. The upper L_3 state is denoted by $L_3^{(2)}$. The heavy-mass band responsible for the 2-eV absorption edge corresponds to $X_5\, Z_2\, W_{1'}\, Q_+\, L_3^{(2)}$.

well inside the atom and hence functions such as $\langle p|\mathbf{k}\rangle$ and $\langle s|\mathbf{k}\rangle$ are readily computed in terms of free-atom wave functions,[18] and are shown in Fig. 1.

The state $|X_{4'}\rangle$ has $m_k=0$. The d states with $|m_k|=0$ or 1 are X_1 and X_5, respectively.[13] Consider the latter transitions

$$\langle X_5|p_t|X_{4'}\rangle = -2C_X^{-1}\langle p|\mathbf{X}\rangle\langle d|p_t|3p\rangle. \quad (2.3)$$

The right-hand side involves known functions as well as the matrix element $\langle d|p_t|3p\rangle$ which we seek to determine.

Phillips has shown[11] how to obtain the left-hand side of Eq. (2.3) directly from eigenvalues obtained in a "first-principles" calculation. This is done by modifying conventional $\mathbf{k}\cdot\mathbf{p}$ perturbation theory to take account of the resonant character of the d states. He finds that the transverse masses of X_5 and $X_{4'}$ should be represented as

$$\frac{m}{m_t}(X_5) = -S + \frac{2}{m}\frac{|\langle X_5|p_t|X_{4'}\rangle|^2}{E(X_5)-E(X_{4'})}, \quad (2.4)$$

$$\frac{m}{m_t}(X_{4'}) = 1+R+\frac{2}{m}\frac{|\langle X_5|p_t|X_{4'}\rangle|^2}{E(X_{4'})-E(X_5)}, \quad (2.5)$$

where S is a term arising from the finite (tight-binding) width of the d bands alone, while R represents a correction arising from the orthogonality terms in our model Hamiltonian. He makes the ansatz $R=S$ (partial-sum rule), which is consistent with the results of Burdick's calculation.[5]

We have determined the transverse effective masses from Burdick's eigenvalues by plotting

$$[E(\mathbf{X}+\delta k_t)-E(\mathbf{X})]/(\delta k_t)^2 = A+B(\delta k_t)^2+\cdots \quad (2.6)$$

and extrapolating to $\delta k_t=0$. This gives the results shown in Table I. It is seen that the off-diagonal hybridization terms involving $|\langle X_5|p_t|X_{4'}\rangle|^2$ contribute roughly half of the effective masses. Thus on the basis of this factor the oscillator strength is roughly half as great at X as previously estimated.[15]

When we consider $\Delta m=0$ "longitudinal" transitions, we encounter matrix elements between the d states and plane-wave states of the form $\mathbf{k}\langle d|\mathbf{k}\rangle$. These are easily evaluated in terms of the orthogonality form factors $M_d(k)$ introduced into the model Hamiltonian.[10] Also required are matrix elements between orthogonalized plane waves (OPW's). In this case because $\mathbf{p}$ is parallel to $\mathbf{k}$, plane-wave matrix elements of the form $\langle\mathbf{k}|\mathbf{p}|\mathbf{k}\rangle$ are nonzero [in contrast to the $|\Delta m|=1$ case of Eq. (2.3)]. Previous calculations[17] have shown that such terms dominate, and the s and p core orthogonality corrections can be neglected. In our case we also have d orthogonality corrections. These can be quite large; for example, at X they increase the oscillator strength for the (unphysical) transition $X_{4'} \rightarrow X_1$ from a free-electron value of 46 to 64 eV; the corresponding correction for the (physical) transition $L_{2'} \rightarrow L_1$ is only from 35 to 43 eV. To allow for the possibility of such corrections we have retained the orthogonality corrections to conduction-band → conduction-band matrix elements.

The situation at $\mathbf{L}$ is somewhat more complex. The conduction-band state $L_{2'}$ still corresponds to $m_k=0$, as does the d state L_1. From a preceding paper[13] we see that the upper L_3 state is 92% $|m_k|=1$, while the lower L_3 state is 8% $|m_k|=1$. The appropriate decomposition of the effective masses is indicated in Table II. In order to account for the transverse effective masses of the lower $L_3^{(1)}$ state it is necessary to invoke interactions with $L_{3'}$ states which lie approximately 2.0 Ry above the d bands. These interactions—which are of no direct interest—modify the oscillator strength $|\langle L_3^{(2)}|p_t|L_{2'}\rangle|^2$ by only about 2%.

We are now in a position to check internally the consistency of our procedure for avoiding explicit determination of the d states. From the matrix elements $|\langle X_5|p_t|X_{4'}\rangle|^2$ and $|\langle L_3^{(2)}|p_t|L_{2'}\rangle|^2$ we obtain two independent expressions for $\langle d|p_t|3p\rangle$ as in Eq. (2.3). Eliminating normalization and orthogonality factors in Eq. (2.3), we obtain from the effective masses at X

TABLE I. Decomposition of m/m_t for the levels of p and d ($m=\pm1$) character ($X_{4'}$ and X_5) at X. The results of Burdick's APW calculation (Ref. 5) are listed in row 1. The nomenclature for the remaining rows is that used by Phillips (Ref. 11).

	$X_{4'}$	X_{51}	X_{52}
Burdick	+2.53	−1.53	0.0
Kinetic energy	+1.00	···	···
Hydbridization	+0.86	−0.86	0.0
d-band width (S)	···	−0.67	0.0
Orthogonalization (R)	+0.67	···	···

[18] F. Herman and S. Skillman, *Atomic Structure Calculations* (Prentice-Hall, Inc., Englewood Cliffs, New Jersey, 1963).

shown in Table I the result

$$\frac{2}{m}|\langle 3d,\ m_k=1|\ p_t|\ 3p,\ m_k=0\rangle|^2=36\ \text{eV}. \quad (2.7)$$

The corresponding result at L is 34 eV. The difference of less than 10% provides an internal check on the consistency of our procedures for using effective masses to determine oscillator strengths.

Having verified the consistency of our procedure at X and L, we can interpolate and obtain oscillator strengths throughout the Brillouin zone between all the occupied levels and all the unoccupied levels. This interpolation is based on $3s$ and $3p$ orthogonality form factors for the free atom, the $3d$ orthogonality form factor determined by our interpolation scheme, as well as the model eigenvectors in Eq. (2.1). The new element is the $3d$-$3p$ oscillator strength discussed in Eq. (2.7); the assumption of d isotropy plays an important role in determining this matrix element for all $\mathbf{k}$.

We can anticipate that the oscillator strengths so determined will be complicated functions of m, n, and $\mathbf{k}$. This is illustrated in Fig. 2 by plotting the values of $2P_{mn}^2(\mathbf{k})/m$ for transitions from the lowest five bands to the sixth band around the edge $XZWQL$ of the Brillouin zone. It appears that the convenient assumption that these quantities are constant over an appreciable solid angle[15] (an assumption whose limitations were recognized and discussed by CEP[15]) is not bad for the smaller square faces (XZW) of the Brillouin zone, but that it is quite poor for the larger hexagonal faces (LQW) where m_k is not a good quantum number.

The oscillator strengths shown in Fig. 2 were obtained using the model parameters[10] appropriate to the band structure of Cu calculated by Segall[6] from an l-dependent potential. In order to test the sensitivity of these oscillator strengths to small changes in potential we repeated the calculation using the model parameters[10] appropriate to the l-independent Chodorow potential.[5,6]

TABLE II. Decomposition of m/m_t for the levels of p and d ($m=0$) character at L. The values in the row labeled Burdick are taken from a graphical fit to the results of Ref. 5. The nomenclature for the remaining rows follows that of Phillips (Ref. 11), with the exception of the last row. Here the discrepancy between the magnitude of the hybridization term obtained from Mueller's interpolation scheme (Ref. 10) and that required to fit the APW masses is attributed to the nearby L_3' states (of p symmetry) which are omitted from the interpolation scheme. Fortunately the $L_3^{(1)}$ states contribute little to the optical spectrum in any case, so that this discrepancy is of little importance.

	$L_{2'}$	$L_3^{(2h)}$	$L_3^{(2l)}$	$L_3^{(1h)}$	$L_3^{(1l)}$
Parity	(−)	(+)	(−)	(+)	(−)
Burdick	+3.19	−0.03	−2.11	+0.30	−0.64
Kinetic energy	1.00	···	···	···	···
Hybridization	1.77	0.0	−1.66	0.0	−0.11
d-band width (S)	···	−0.03	−0.42	+0.30	−0.16
Orthogonalization (R)	0.42	···	···	···	···
Missing term (L_3' states)	···	···	−0.03	···	−0.37

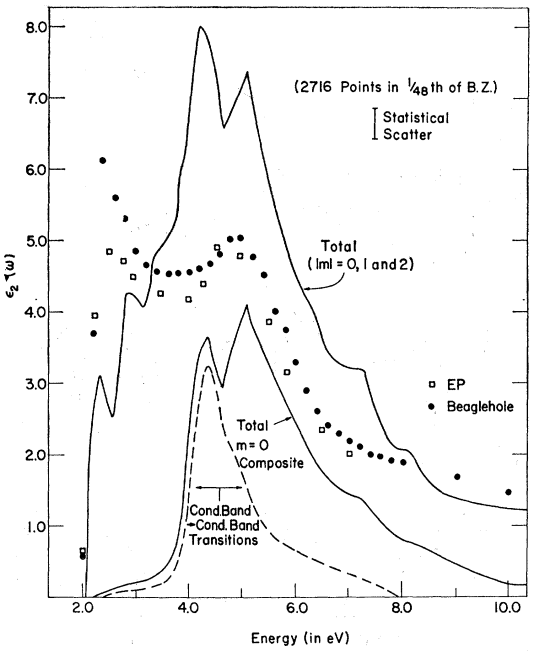

FIG. 3. A plot of the interband contribution to $\epsilon_2(\omega)$ in the range $1.5\leq\hbar\omega\leq10$ eV for Cu. The experimental data shown are those of Refs. 14 and 19. The original Monte Carlo sample of 2716 nonequivalent points in 1/48th of the Brillouin zone yielded a histogram with an rms statistical error in an energy interval of 0.01 Ry as indicated. This histogram was then smoothed, taking into account the analytic singularities discussed in the text; the smoothed curves should therefore be more accurate than the original histogram. The theoretical curve marked "total" includes all d-band → conduction-band and conduction-band → conduction-band transitions. The lower theoretical solid curve is a composite of the conduction-band → conduction-band transitions (which are important mainly in the neck region near $L_{2'}\rightarrow L_1$) and the d-band ($m=0$) → conduction-band transitions shown in Fig. 4. The dashed curve shows the contribution of only conduction-band → conduction-band transitions.

Virtually identical results were obtained, except for the branch involving $\Delta m=0$ transitions from hybridized d states (such as X_1 or L_1) to p-like conduction states ($X_{4'}$ or $L_{2'}$). For these transitions the parameters appropriate to the l-independent potential gave results 50% greater than those shown in Fig. 2.

The extraordinary sensitivity of the oscillator strengths of these transitions to small changes in the parameters of the model Hamiltonian arises from the fact that the amplitude for transitions between the hybridized d-s states and p conduction states is a sum of two interfering terms. The extent to which these terms cancel greatly affects our calculated oscillator strengths, and this degree of cancellation cannot be determined accurately within the framework of the model Hamiltonian. It should be decided by a careful study of *ab initio* matrix elements, bearing in mind that these, too, will be very sensitive to numerical approximations or to small changes in crystal potential.

Although the magnitude of these matrix elements has not been determined accurately, comparison of the results for the two sets of model parameters suggests that

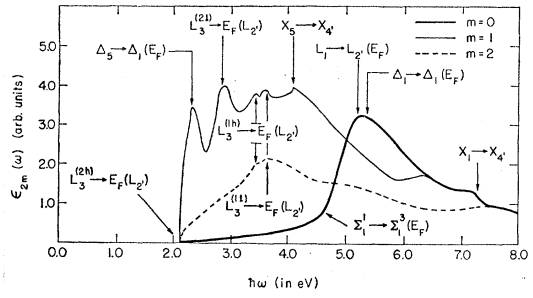

FIG. 4. Here are decomposed the contributions to ϵ_2 of d-band $\rightarrow$ conduction-band transitions, with each initial state divided fractionally into $|m|=0$, 1, and 2 states. It was anticipated that most of the spectral structure would be found in the $|m|=0$ and 1 subbands, and this proves to be the case. Analytic singularities associated with critical points or osculation points at the Fermi surface are specifically marked; the corresponding transitions are shown in the band structure in Fig. 5.

the relative k-dependence is given approximately correctly by our calculations. In the presentation of our results, transitions from hybridized states to conduction band states are labelled $m=0$. It is understood that the magnitude of the contribution of these transitions to ϵ_2 may be in error by as much as 50%. We believe the other types of transitions have been treated with an accuracy of about 10%. Finally, to obtain all our results we have used the parameters of the model potential appropriate to the l-independent potential.

III. INTERBAND SPECTRUM

We show in Fig. 3 the complete smoothed spectrum for $\epsilon_2(\omega)$ calculated in the Hartree approximation. The original histogram with energy intervals of 0.01 Ry was formed from 2716 points randomly distributed throughout the Brillouin zone. By making the assumption that all the conduction-band states correspond to $m_k=0$, we can decompose this spectrum into contributions from d states, each of which has a certain fraction of its probability density associated with $|m_k|=0$, 1, or 2. This decomposition is shown in Fig. 4. It is useful for understanding structure in the complete spectrum.

At this point we pause to analyze analytic singularities that may arise in the interband spectrum of a metal. These are of two kinds: firstly, critical points where

$$\nabla_{\mathbf{k}}[E_f(\mathbf{k})-E_i(\mathbf{k})]=0, \qquad (3.1)$$

where i and f label initial and final states. The second kind of singularity[15] arises from shells near the Fermi surface, where the exclusion principle plays a decisive role. These singularities, which produce a discontinuity in slope of $\epsilon_2(\omega)$, occur because there are points in k space where the surface of constant interband energy osculates the Fermi surface. Such points always occur at the intersection of the [100], [111], and [110] symmetry axes with the Fermi surface. If the points are closely spaced in energy (as they are here for the [100] and [110] directions), one may obtain a sharp rise in absorption over a narrow energy range, corresponding almost to an absorption edge.

From Fig. 4 we see that there is a sharp edge at 2.1 eV which is associated primarily with the $m=1$ d bands. This edge is followed by a second one at 2.9 eV, also associated with $m=1$ states. The first edge corresponds to the "heavy mass" or nearly flat highest d band, denoted by $X_5^{(h)}Q_+W_{1'}$ and $L_3^{(2h)}$ at the principal symmetry points. The second edge is associated with the "light mass" mass $X_5^{(l)}Q_-W_3$ and $L_3^{(2l)}$. See Fig. 5 for the $Q_+ \rightarrow Q_-(E_F)$ transitions denoted equivalently by $L_3^{(2h)} \rightarrow E_F(L_{2'})$ and $L_3^{(2l)} \rightarrow E_F(L_{2'})$ in Fig. 4.

Further very weak structure is seen in the $m=1$ band. Because of histogram scatter, this structure would not have been resolved had we not expected it on analytic grounds. This remark applies also to the $X_5 \rightarrow X_{4'}$ saddle-point edge at 4.1 eV, which was previously supposed[15] to be responsible for the second peak in Cu. Our calculations show conclusively that this is not the case.

If m_k were a good quantum number, the $m=2$ subbands would contribute almost nothing to $\epsilon_2(\omega)$. However, as we noted in a preceding paper,[13] the largeness of the covalent d-d mixing makes m_k a poor quantum number throughout much of the Brillouin zone. Nevertheless, the $m=2$ states still should not contribute much *structure* to $\epsilon_2(\omega)$; and this is seen to be the case in Fig. 4, where the $m=2$ contribution is broad and featureless apart from weak edges associated with $L_3^{(l)} \rightarrow E_F(L_{2'})$ transitions.

Transitions with $\Delta m_k=0$ are of two types. The d band ($m_k=0$) $\rightarrow$ conduction-band transitions are shown in Fig. 4. (As remarked at the end of Sec. A, the scale of these transitions is not determined to better than 50%.) These start, as shown in Fig. 5, from the lowest d band $X_1Z_1Q_+L_1$ and go to the conduction band; the shell near the Fermi surface produces a sharp edge around 5.2 eV. The second type of transition is conduction band $\rightarrow$ conduction band. Although the phase space of the necks associated with the $L_{2'} \rightarrow L_1$ saddle-point edge is small, the large oscillator strength ($\approx$40 eV) of these transitions gives rise to a strong edge at the $L_1-L_{2'}$ energy difference. The contribution of both types of $\Delta m=0$ transitions is shown separately in Fig. 3.

It is evident from Fig. 3 that the second peak in the experimental spectrum[14,19] near 4.8 eV arises from $m=0$ transitions, and not from $m=1$ transitions near $X_5 \rightarrow X_{4'}$, as had previously been supposed.[15] If we suppose that the lowest d band is strongly lifetime-broadened (principally by Auger transitions of the final-state hole to higher d states), then the experimental peak at 4.8 eV should be identified with the $L_{2'} \rightarrow L_1$ peak, while the second theoretical peak at 5.1 eV would be too broad to be resolved. The observed energy difference of 4.8 eV for $L_{2'} \rightarrow L_1$ compares with Burdick's value of 4.5 eV and Segall's value of 5.9 eV.

[19] D. Beaglehole, Proc. Phys. Soc. (London) 85, 1007 (1965); 87, 461 (1966).

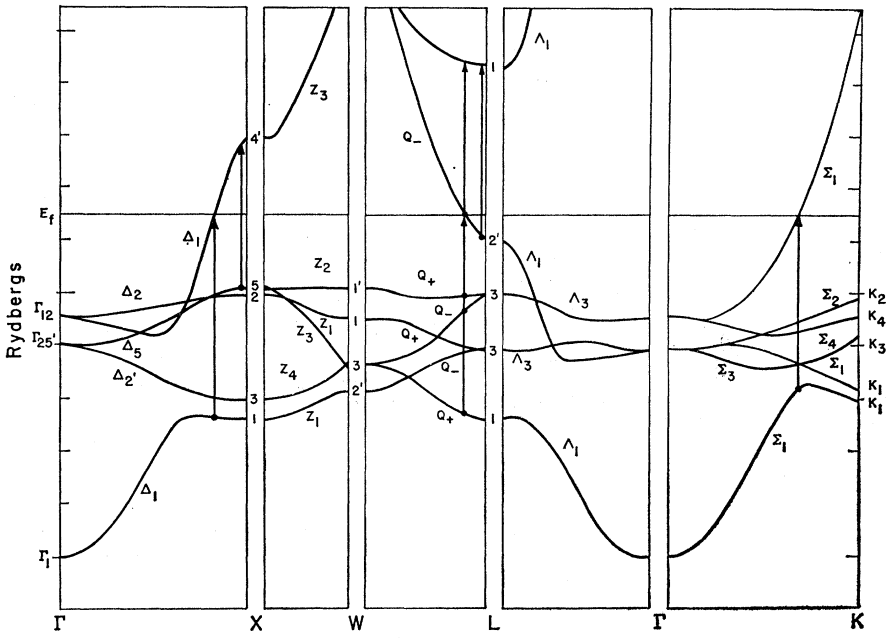

FIG. 5. Direct transitions giving rise to analytic singularities are marked here in the energy bands of Cu (after Burdick, Ref. 5). The electron states are represented by the tips of the arrows, the hole states by the solid circles.

The greatest difference between the theoretical spectrum and the experimental spectrum occurs just above the interband absorption edge. We believe this difference arises because of many-body effects lying outside the simple random-phase approximation for $\epsilon_2(\omega)$ given in Eq. (1.1). We return to these effects in Sec. V.

IV. COMPARISON WITH OTHER WORK

In addition to the work of CEP, other studies of the optical properties of the noble metals have been made by Haga and Okamoto.[16] However, the last-named authors, although they use the same graphical method[20] for evaluating phase-space sums as CEP, and recognize, as did CEP, that oscillator strengths are difficult to determine, cautiously take them as adjustable parameters. By contrast, CEP carry out an absolute calculation of Eq. (1.1) which can be compared directly to experiment. We examine their calculation critically in this section. The analysis reveals the limitations of simplified calculations of the optical spectra of crystals.

CEP begin by assuming that the interband spectrum is dominated by transitions from the highest d band (which corresponds to the heavy-mass d band near X_5 and $L_3^{(2)}$) to the lowest conduction band. In our nomenclature this is one of the two $m=1$ bands labeled by X_5 Z_2 $W_{1'}$ Q_+ $L_3^{(2)}$ in Fig. 2. If we neglect the effects of s-d mixing and retain the well-founded approximation of d isotropy, this transition should account for at most one-third of the strength of the interband (momentum matrix element).[2] This point may be verified directly by reference to Fig. 2, which shows that at X the effect of s-d mixing as well as the orthogonality contributions makes the $m=0$ oscillator strength slightly smaller than that of the $m=1$ states, while at L the reverse is true. At W there is strong mixing of the m states, but the total strength of P_{mn}^2 is approximately conserved. Thus the absolute calculation of CEP, although it covers the energy range 2.1–4.0 eV, can be expected to yield accurate results only in the range 2.1–2.5 eV, where the heavy-mass band genuinely dominates. Already at 2.8 eV the "light-mass" band represents half the oscillator strength; and near 4 eV, half the oscillator strength comes from the $m=0$ transitions near $L_{2'} \rightarrow L_1$, which are also omitted by CEP.

Now consider specifically the energy range 2.1–2.5 eV, where the heavy-mass band does indeed dominate. To estimate the strength of the edge absolutely, CEP must first determine the oscillator strengths in terms of the matrix elements of p_t between the L_3 states and the $L_{2'}$ state. This they do by using $\mathbf{k}\cdot\mathbf{p}$ perturbation theory, following earlier work,[21] which, however, neglected the orthogonality corrections to the effective mass of conduction-band states. (As we have noted,[11] these corrections can in general lead to large changes in derived values of $|P_{mn}|^2$, e.g., by as much as a factor of 2 for the $X_5 \rightarrow X_{4'}$ transitions. As discussed in Sec. II, these corrections are included in the present calculations.) In the present case the orthogonality correction to $m/m_t(L_{2'})-1$ is 0.42, compared to the hybridization value 1.77, and thus represents a 20% effect.

When we know the off-diagonal hybridization contribution to $m/m_t(L_{2'})$, we can use the effective-mass sum rule

$$\frac{m}{m_t(L_{2'})}=1+R+\frac{2}{m}\sum_{j=L_3}\frac{|\langle L_j|p_t|L_{2'}\rangle|^2}{E(L_{2'})-E(L_3)} \qquad (4.1)$$

[20] J. M. Ziman, Advan. Phys. **10**, 1 (1961).

[21] J. C. Phillips and L. F. Mattheiss, Phys. Rev. Letters **11**, 556 (1963).

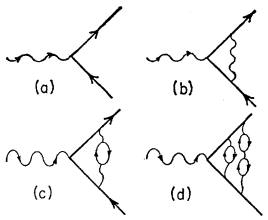

FIG. 6. A sketch of some of the various terms in perturbation theory contribution to optical absorption. The wiggly lines represent the incident photon. In the random-phase approximation used here, the optical absorption is determined by (a), where the electron and hole are treated as noninteracting (Hartree approximation). In (b), (c), and (d) some Coulomb and polarization terms are shown, which taken altogether correspond to vertex corrections associated with electron-hole interactions in the final state. It is suggested that these interactions produce a virtual exciton resonance near 2 eV in Cu.

to determine the matrix elements

$$P_{32'}=\langle L_3|p_t|L_{2'}\rangle, \tag{4.2}$$

which are required to calculate oscillator strengths. With two doubly degenerate L_3 states there are four matrix elements of the type Eq. (4.2) to be calculated. Using group theory one can reduce these four elements to two, one for each of the L_3 states, and using the assumption of d isotropy one can express the two elements in terms of one, when the L_3 model eigenvectors are known from the tight-binding part of the model Hamiltonian.

First consider the reduction by group theory.[22] Orient p_t along the line $Q=LW$; the doubly degenerate L_3 basis states can be classified according to whether they have even or odd parity with respect to the group of Q. Then $L_{2'}$ and p_t have odd parity, as do the light-mass L_3 states, while the heavy-mass state (which becomes Q_+ along LW) has even parity. We immediately obtain

$$|\langle L_{2'}|p_t|L_3^{(2h)} \text{ or } L_3^{(1h)}\rangle|^2=0, \tag{4.3}$$

compared with the result of CEP [see their Eq. (13)] which states

$$|\langle L_{2'}|p_t|L_3^{(h)}\rangle|^2=|\langle L_{2'}|p_\perp|L_3^{(l)}\rangle|^2. \tag{4.4}$$

The difference between Eqs. (4.3) and (4.4) is one of definition. By $p_\perp$ CEP mean *both* components of $\mathbf{p}$ transverse to ΓL. This convention differs from the more common one used here. Our convention is based on the derivation of Eq. (4.1) by $\mathbf{k}\cdot\mathbf{p}$ perturbation theory, where $\mathbf{k}$ of course lies in a specific direction (e.g., along Q). In order to account for all components of $\mathbf{p}$, we multiply our final result by $\frac{1}{3}$; they multiply their result by $\frac{2}{3}$. Thus apart from the 20% correction represented by orthogonality terms, our results would agree at L if CEP had carried out the second reduction (discussed below) correctly. At X, however, because of orthogonality corrections their oscillator strength for $X_5\rightarrow X_{4'}$ is too large by a factor of 2.

The second reduction lies in making use of the model eigenvectors to determine the constant C:

$$|\langle L_3^{(2h)}|p_t|L_{2'}\rangle|^2=C|\langle L_3^{(1h)}|p_t|L_{2'}\rangle|^2. \tag{4.5}$$

Here the quantum number m_k is useful. It states[13] that because the L_{32} state is 92% $m_k=1$, while the L_{31} state is only 8% $m_k=1$, the value of C is about 11. This contrasts with the ad hoc assumption of CEP that $C=1$. The large value of C arises because of the trigonal axial symmetry of L, which makes m_k almost a good quantum number.

We conclude this section with some remarks about the appropriateness for this problem of the "eight cone" model originally constructed by Ziman[20] for application to transport problems. If all the d bands were flat, and all the oscillator strengths were constant over the L cones, this model would yield statisfactory results for the optical spectrum. Reference to Fig. 2 and to Fig. 5 will show that these conditions are far from being satisfied, which implies that a graphical approach to this problem is not warranted.

V. CONCLUSIONS: MANY-BODY EFFECTS

We return now to Fig. 3. Two sets of experimental data[14,19] are compared with the theoretical curve. Above 4 eV there is generally good agreement between the three curves; the second peak near 5 eV is identified with conduction-band → conduction-band transitions in the neck region near $L_{2'}\rightarrow L_1$, and there is evidence near 7 eV that the faint structure resolved by Beaglehole[19] may be due to $X_1\rightarrow X_{4'}$ transitions. In general it appears that Beaglehole's data, which show somewhat sharper structure (especially near 2 eV), may be somewhat better, because of better surface preparation.

Our assignment of the second peak to $L_{2'}\rightarrow L_1$ transitions agrees with that proposed by Beaglehole.[19,23] Our calculations also explain the absence of a second peak in Ag, although two peaks are seen in Au. The Ag d bands are shifted downwards, below the Fermi energy, by 2 eV relative to Cu and to Au. In the CEP model, this would simply shift the entire interband spectrum 2 eV higher in energy. With our interpretation, however, one would expect the $L_{2'}\rightarrow L_1$ peak (now much smaller, because the neck in Ag is smaller) approximately to coincide with the $L_2^{(2)}\rightarrow L_{2'}$ edge near 4 eV. Thus in Ag only one peak is expected, and only one is observed.

In view of the good absolute agreement at higher energies between our calculated spectrum and the observed spectrum, we feel justified in suggesting that the strong peak in the observed spectrum near 2 eV should be identified as a virtual exciton resonance. The Coulomb interaction in the final state between the excited electron in the conduction band and the hole in the d band is of

[22] L. P. Bouckaert, R. Smoluchowski, and E. Wigner, Phys. Rev. **50**, 58 (1936). See the discussion on p. 67 for the importance of orienting Pt along $Q=LW$.

[23] C. N. Berglund and W. E. Spicer, Phys. Rev. **136**, A1030 (1964); **136**, A1044 (1964).

course strongly screened by many-body correlations, so that it is short-range in character. When the interaction element U_{sd} lies below a certain critical strength, no bound exciton is formed, but a virtual (resonant) state is found above the edge, which appears as a peak in the spectrum. It appears that this is what is happening in Cu; note that another mechanism would be required to produce a weak peak below the absorption edge, and below the virtual exciton peak. [We believe that the weak peak which has been observed[24] just below the edge in Ag and in Au is associated with surface states, possibly induced by impurities (oxide) on the surface.]

A general formalism for treating exciton effects in metals has not appeared,[25,26] but we will sketch here how the calculation would proceed. In the language of field theory, we are concerned with vertex corrections to the process of direct absorption indicated in Fig. 6(a), which has been evaluated for Cu in this paper. Some of the vertex corrections are sketched in Fig. 6(b)–6(d). If we describe the dynamical screened Coulomb interaction in the final state by a single "central-cell" parameter U_{sd}—an approximation which is appropriate considering our limited ability to calculate such parameters even in the much simpler situation of a free-electron gas—then by using a resolvent formalism[27,28] we can obtain an effective interband density of states by calculating $|\Phi(0)|^2$, where $\Phi(\mathbf{R})$ is the Wannier envelope function obtained by solving the resolvent equations. Thus we obtain the optical spectrum in terms of a single many-body parameter, U_{sd}. (Calculations along these lines have already been carried out for Xe using a long-range Coulomb interaction.[29]) Adjustment of U_{sd} to produce the virtual exciton resonance determines this many-body parameter.

It is our view that proceeding in this manner, i.e., first calculating the spectrum accurately in the one-electron, random-phase approximation, and then comparing to experiment, offers an interesting way to obtain direct information concerning many-body interactions that may not be obtainable from Fermi-surface studies alone. We, therefore, hope to apply this technique to other noble and transition metals when our knowledge of the one-electron band structures warrants it.

We close with some remarks about the optical spectrum of Ni, which is as yet little understood. Because, on going from Cu to Ni, the d bands are shifted upwards relative to the s-p bands, one at first expects the interband $d \rightarrow$ conduction-band spectrum to be similar to Cu, but shifted to lower energies by about 1.5 eV. At energies below 3 eV this seems to be the case, but the peak at 4.8 eV in Cu is shifted[30] only to 4.4 eV in Ni. Note also that in Ni the occupied neck regions near $L_{2'}$ are much smaller than in Cu.[31]

According to the present calculation, the 4.8-eV peak in Cu may arise predominantly from $L_{2'} \rightarrow L_1$ type transitions, while the 4.4-eV peak in Ni could arise primarily from $L_1 \rightarrow L_2'$, i.e., hybridized $d \rightarrow$ Fermi-surface transitions (of the $m=0$ type, see Fig. 4). The two peaks are approximately of the same height, but this could be due to the fact (discussed at the end of Sec. II) that the oscillator strengths of the $m=0$ type transitions are so sensitive to small changes in crystal potential, and increase significantly from Cu to Ni.

ACKNOWLEDGMENTS

We are grateful to Dr. R. Sandrock for checking the calculations and to Dr. D. Beaglehole for comments on the manuscript.

[24] M. Garfinkel, J. J. Tiemann, and W. E. Engeler, Phys. Rev. **148**, 695 (1966).

[25] Some modification of the usual Wannier functions (see Ref. 26) is required in metals to be consistent with the exclusion principle. This modifies the interpretation of the meaning of U_{sd}, which now corresponds to a matrix element between spread-out states which do not necessarily resemble atomic states.

[26] R. J. Elliott, Phys. Rev. **108**, 1384 (1957).

[27] J. C. Slater and G. F. Koster, Phys. Rev. **95**, 1167 (1954).

[28] J. Callaway, J. Math. Phys. **5**. 783 (1964).

[29] J. Hermanson (to be published).

[30] H. Ehrenreich, H. R. Philipp, and D. J. Olechna, Phys. Rev. **131**, 2469 (1963).

[31] J. C. Phillips, Phys. Rev. **133**, A1020 (1964).